Locale and chemistry of spermine binding in the archetypal inward rectifier Kir2.1

Harley T. Kurata,[1] Emily A. Zhu,[2] and Colin G. Nichols[2]

[1]Department of Anesthesiology, Pharmacology, and Therapeutics, University of British Columbia, Vancouver, British Columbia V6T 1Z3, Canada

[2]Department of Cell Biology and Physiology, and Center for Investigation of Membrane Excitability Disorders, Washington University School of Medicine, St. Louis, MO 63110

Polyamine block of inwardly rectifying potassium (Kir) channels underlies their steep voltage dependence observed in vivo. We have examined the potency, voltage dependence, and kinetics of spermine block in dimeric Kir2.1 constructs containing one nonreactive subunit and one cysteine-substituted subunit before and after modification by methanethiosulfonate (MTS) reagents. At position 169C (between the D172 "rectification controller" and the selectivity filter), modification by either 2-aminoethyl MTS (MTSEA) or 2-(trimethylammonium)ethyl MTS (MTSET) reduced the potency and voltage dependence of spermine block, consistent with this position overlapping the spermine binding site. At position 176C (between D172 and the M2 helix bundle crossing), modification by MTSEA also weakened spermine block. In contrast, MTSET modification of 176C dramatically slowed the kinetics of spermine unblock, with almost no effect on potency or voltage dependence. The data are consistent with MTSET modification of 176C introducing a localized barrier in the inner cavity, resulting in slower spermine entry into and exit from a "deep" binding site (likely between the D172 rectification controller and the selectivity filter), but leaving the spermine binding site mostly unaffected. These findings constrain the location of deep spermine binding that underlies steeply voltage-dependent block, and further suggest important chemical details of high affinity binding of spermine in Kir2.1 channels—the archetypal model of strong inward rectification.

The Journal of General Physiology

INTRODUCTION

Polyamine block of inwardly rectifying potassium (Kir) channels underlies their key functional property of preferential conduction of inward K^+ currents (Ficker et al., 1994; Lopatin et al., 1994, 1995; Fakler et al., 1995). As a rapid and voltage-dependent process, polyamine-mediated inward rectification provides a mechanism for moment-to-moment regulation of K^+ currents in excitable tissues, shaping both the action potential and resting membrane potential in tissues such as myocardium (Bianchi et al., 1996; Lopatin et al., 2000; Priori et al., 2005; Schulze-Bahr, 2005). Akin to the ongoing challenges to understanding voltage-dependent gating of the Kv channel family, development of a molecular description of steeply voltage-dependent polyamine block is an important issue for understanding the fundamental basis of strongly rectifying Kir channel activity.

Appropriate kinetic models describe polyamine block as a multistep process, incorporating sequentially linked "shallow" and "deep" binding steps of polyamines in the Kir pore (Lopatin et al., 1995; Guo and Lu, 2000; Shin and Lu, 2005; Kurata et al., 2007). Structurally, these shallow and deep binding steps are conceptualized as initial weakly voltage-dependent binding, probably in the cytoplasmic domain of the channel, followed by a steeply voltage-dependent step in which spermine migrates to a stable binding site in the inner cavity (Xie et al., 2002; John et al., 2004; Shin et al., 2005; Kurata et al., 2007). This multistep process is manifested in biphasic conductance–voltage relationships at high (~100 μM) spermine concentrations, in which shallow voltage-dependent block is apparent at negative voltages, and a steeply voltage-dependent phase is observed at more depolarized voltages (Xie et al., 2002). Residues critically involved in each step have been identified: mutations that affect the shallow binding step cluster in the cytoplasmic domain (Yang et al., 1995; Kubo and Murata, 2001; Guo et al., 2003; Xie et al., 2003; Fujiwara and Kubo, 2006; Kurata et al., 2007), while the "rectification controller" residue (D172), critical for steep voltage-dependent block, lies at a pore-lining position in the Kir inner cavity (Wible et al., 1994; Shyng et al., 1997). Molecular modeling of electrostatics in the Kir pore (Robertson et al., 2008) indicates that variable long-range effects of charged amino acid side chains are also possible, due to variable dissipation of electric

Correspondence to Harley T. Kurata: harley.kurata@ubc.ca

Abbreviations used in this paper: Kir, inwardly rectifying potassium; MTS, methanethiosulfonate; MTSEA, 2-aminoethyl MTS; MTSET, 2-(trimethylammonium)ethyl MTS; WT, wild-type.

The Rockefeller University Press $30.00
J. Gen. Physiol. Vol. 135 No. 5 495–508
www.jgp.org/cgi/doi/10.1085/jgp.200910253

fields through the protein dielectric versus the aqueous pore. Thus, there need not be a strict boundary defining residues that affect either blocking equilibrium.

An important obstacle to a full explanation of the origins of steep voltage dependence of polyamine block is a concrete description of the stable deep spermine binding site in strongly rectifying Kir channels. We have taken several different approaches to this issue, using the Kir6.2 channel as a model (Kurata et al., 2004, 2006, 2008). In this model system, the N160D mutation (equivalent to the naturally occurring 172D in Kir2.1) is used to introduce strong polyamine sensitivity and steeply voltage-dependent block, as the wild-type (WT) Kir6.2 channel is otherwise very insensitive to polyamines. These studies generated a very consistent indication for the stable binding site for spermine lying deep in the Kir inner cavity between the rectification controller residue and the selectivity filter.

By implication, a similar location is predicted for spermine binding in naturally occurring strong inward rectifiers, but it is of note that certain studies of Kir2.1 have led to alternative interpretations, specifically that the leading end of spermine lies near residue D172 (the rectification controller), and the trailing end lies near Kir2.1 residue M183 on the cytoplasmic side of the inner cavity region (Shin and Lu, 2005; Xu et al., 2009). In the present study, we directly probed this possibility by examining the effects of modification of Kir2.1 inner cavity residues by different cationic methanethiosulfonate (MTS) reagents. We demonstrate that at Kir2.1 position 176C, one helical turn below the rectification controller residue, effects of modification depend dramatically on detailed properties of the modifying reagent. 2-Aminoethyl MTS (MTSEA) significantly reduces the potency of spermine binding. In contrast, 2-(trimethylammonium)ethyl MTS (MTSET; a quaternary ammonium carrying a similar +1 charge) has little effect on steady-state spermine block, suggesting that cationic substituents at position 176 do not directly disrupt the stable spermine binding site. Most importantly, MTSET modification of position 176 dramatically slows spermine unbinding. These findings offer straightforward and definitive constraints on the location of spermine binding in Kir2.1: steeply voltage-dependent block results from binding above position 176. In so doing, this study provides new tests for validation of current kinetic models of polyamine block, and suggests important chemical features of the spermine binding site.

MATERIALS AND METHODS

Kir2.1 channel constructs

All cysteine mutations were introduced using the Quickchange method (Agilent Technologies) on a previously described "IRK1J" background construct, in which six cysteines have been removed (C54V, C76V, C89I, C101L, C149F, and C169V) to abolish reactivity to cysteine-reactive probes (Lu et al., 1999; Chang et al., 2005). Six endogenous cysteines remain in the construct (C122, C154, C209, C311, C356, and C375). Throughout the text, this nonreactive Kir2.1 background is referred to as Kir2.1*. The Kir2.1* template DNA was provided by R.-C. Shieh (Institute of Biomedical Sciences, Taipei, Taiwan). Dimeric constructs were generated by introduction (using PCR) of overlapping sequences encoding a six-glycine linker at the C terminus of the leading dimer subunit ("front half") and the N terminus of the trailing dimer subunit ("back half"). Subsequent PCR amplification of the front half and back half subunit sequences together generated a linked construct due to overlapping linker sequences that was subcloned into the pcDNA3.1(−) vector.

Electrophysiology

COSm6 cells were transfected with ion channel cDNAs (with mutations as described) and pGreenLantern GFP (Invitrogen) using the Fugene 6 transfection reagent. Patch clamp experiments were made at room temperature using a perfusion chamber that allowed for the rapid switching of solutions. Data were typically filtered at 1 kHz, digitized at 5 kHz, and stored directly on computer hard drive using Clampex software (Axon Inc.). Higher filter and sampling frequencies were used when recording faster kinetics. The standard pipette (extracellular) and bath (cytoplasmic) solution used in these experiments had the following composition: 140 mM KCl, 1 mM EGTA, 1 mM K_2-EDTA, and 4 mM K_2HPO_4, pH 7.3. 50- and 300-mM K solutions were also prepared by changing the concentration of KCl (buffer, EGTA, and EDTA concentrations were maintained constant). Spermine was purchased from FLUKA chemicals (Sigma-Aldrich). MTSEA and MTSET (Toronto Research Chemicals) were dissolved in the standard recording solution on the day of experiments to make a 10-mM stock, which was stored on ice. Working dilutions for channel modification were prepared and used immediately.

Kinetic model of spermine block in Kir2.1

Throughout the text, equilibrium properties of spermine block are fit with a previously described kinetic model (Shin and Lu, 2005; Kurata et al., 2007). The model comprises two sequentially linked blocking steps described by two voltage-dependent equilibrium constants, as shown in Scheme 1.

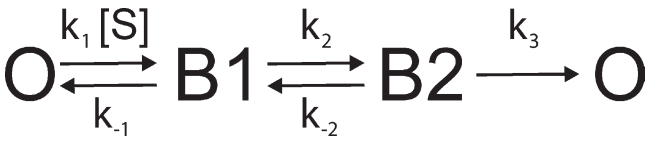

(SCHEME 1)

The shallow binding step (O-B1) describes the weakly voltage-dependent binding of spermine. The deep binding step (B1-B2) describes the entry of spermine from the shallow binding site into a stable deep binding site. The deep binding step involves movement of a significant amount of charge and is steeply voltage dependent. The rate constant k_3 describes a permeation step conceptualized as "punch through" of the blocker through the selectivity filter, a very slow process that is virtually inconsequential at the high concentrations of spermine used in the present study (Guo and Lu, 2000; Kurata et al., 2007). If the permeation step k_3 is ignored, an algebraic description of steady-state open probability is very straightforward: $P_{open} = 1/(1 + K_1[spm] + K_2K_1[spm])$, where [spm] is the concentration of spermine or another blocker, $K_1=k_1/k_{-1}$, and $K_2=k_2/k_{-2}$. Each equilibrium constant or rate constant is assigned a specific effective valence (zδ) to describe the

voltage dependence of each transition: $K_x(V) = K_x(0\ mV)e^{z\delta FV/RT}$ or $k_x(V) = k_x(0\ mV)e^{z\delta FV/RT}$. For rate constants k_x, the exponent is positive for forward/blocking transitions and negative for reverse/unblocking transitions. The equation for P_{open} was fit to experimental data using Microsoft Solver.

Kinetics of spermine block were simulated using the "Q-matrix method" (Colquhoun and Hawkes, 1995). Matrix Q was constructed such that each element (i,j) was equal to the rate constant from state i to state j, and each element (i,i) was set to be equal to the negative sum of all other elements in row i. State occupancy at time t was calculated as $p(t)=p(0)e^{Qt}$, where p(t) is a row vector containing elements corresponding to the occupancy of each state in the model at time t. All tasks required for solving these equations were performed in MathCad 2000 (Parametric Technology Corporation).

In this particular model of Kir2.1, kinetic measurements of block and unblock are linked to model parameters with the following logic. It is assumed that the blocking rate (which empirically has very weak voltage dependence) is limited by the O-B1 transition (k_1) at depolarized voltages, whereas the unblocking rate (which has stronger voltage dependence) is limited by the B2–B1 transition (k_{-2}). Where required, the remaining rates (k_{-1} and k_2) were determined based on the defined relationships between the fitted equilibrium constants (K1 and K2) and the experimentally measured rates (k_1 and k_{-2}).

Online supplemental material

Extensive supplemental material has been included to describe the relationship between the kinetic model and the experimental data. An initial section is included to illustrate how different model parameters affect the predicted properties of spermine block. Section I includes simulated g-V predictions for incremental changes of the shallow (K1) and deep (K2) equilibria, and each voltage dependence (Fig. S1). Section II includes a detailed description of how the model accounts for changes in the kinetics of spermine block after MTSET modification of position 176C (Figs. S2 and S3). Section III is included to describe considerations of interactions between permeant ions, blockers, and MTS adducts in this experimental system (Fig. S4). The online supplemental material is available at http://www.jgp.org/cgi/content/full/jgp.200910253/DC1.

RESULTS

Tandem dimeric constructs of a nonreactive Kir2.1 background channel

We generated a set of linked dimers (Fig. 1 A) of a previously described (Lu et al., 1999; Chang et al., 2005) nonreactive Kir2.1 construct (Kir2.1*), which has six endogenous cysteines mutated and is not responsive to the application of cytoplasmic MTSEA or MTSET. Six endogenous cysteines remained in each channel subunit (see Materials and methods). Neither dimeric linking of constructs nor the introduction of cysteines at position 169 or 176 had any significant effect on the properties of spermine block, and spermine block was also unaltered after exposure of the background Kir2.1*-dimer construct to MTS reagents (Fig. 1 B). Hence, the Kir2.1*-dimer background channel was deemed a suitable model for characterization of polyamine block of Kir2.1. As observed in WT Kir2.1 channels, multiphasic steady-state properties of spermine block are apparent at higher spermine concentrations (~100 μM), but the shallow component is not obvious at lower (~1 μM or less) concentrations. In our initial characterization (Figs. 2–4), we measured block by 100 μM spermine because both the shallow and steep voltage-dependent

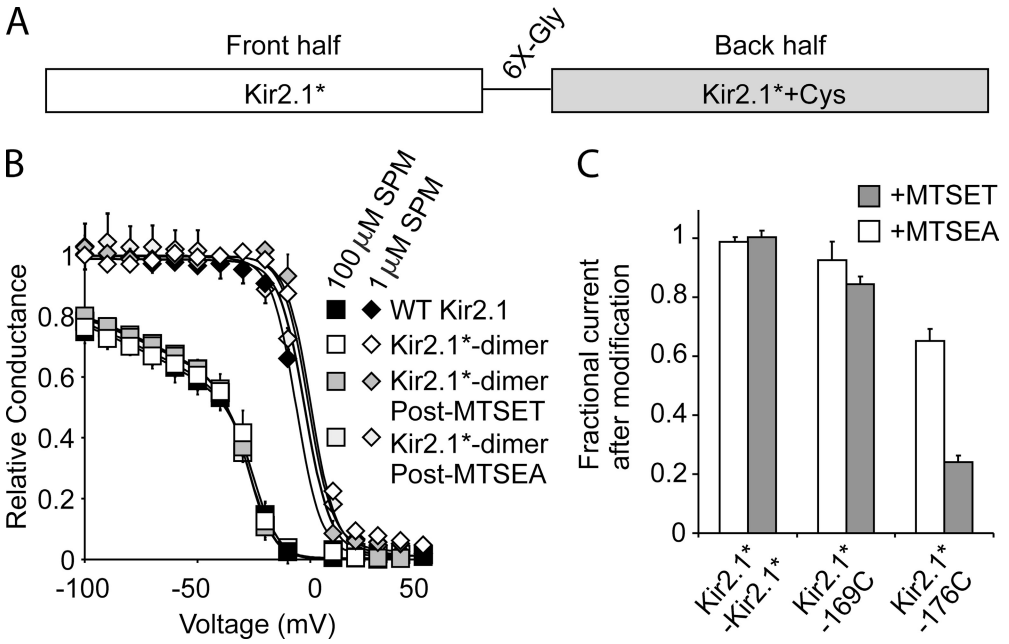

Figure 1. Dimeric Kir2.1* constructs for the introduction of inner cavity cysteines. (A) Dimeric constructs were generated by fusing two copies of Kir2.1* using a 6X-glycine linker introduced by PCR. In all dimeric constructs, the front half comprises the background nonreactive Kir2.1* channels, and the back half comprises a cysteine-substituted Kir2.1* channel. (B) Steady-state spermine block was examined in 1 and 100 μM spermine by pulsing membrane voltage between −100 and +50 mV in 10-mV steps. Spermine block in Kir2.1* dimer channels is similar to spermine block in WT Kir2.1 and is unaffected by exposure to MTS reagents. Mean data are fit with a three-state model described in Materials and methods. (C) Use of dimeric cysteine constructs ensures modest current reduction in cysteine-substituted Kir2.1* dimers after exposure to MTSEA or MTSET, although modification by MTSET causes more dramatic current reduction at both positions examined (169C and 176).

components of spermine block can be resolved (see supplemental text and Fig. S1).

Dimeric constructs comprised the Kir2.1* background subunit linked by six glycines to the N terminus of a cysteine-substituted Kir2.1* subunit (Fig. 1 A). Cysteines were introduced at two pore-lining sites in the Kir2.1 inner cavity, "above" (169C) or "below" (176C) the rectification controller residue (D172). Modification of either substituted cysteine resulted in reduced K^+ current in blocker-free conditions, and the extent of current reduction depended on the cysteine position and the modifying reagent (Fig. 1 C). At both positions examined, MTSET was more disruptive of channel current than MTSEA, and modification of position 176C caused more significant current reduction than modification of position 169C. In homomeric cysteine-substituted channels, modification causes very significant current reduction (especially at position 176C) and would preclude the determination of spermine block in modified channels. The strategy of linking channels in tandem, such that only two cysteines are modified, limits the extent of current reduction after modification and leaves measurable currents after the introduction of positive charges in the inner cavity.

MTSEA and MTSET modification of position 169C

We characterized the effects of both MTSEA and MTSET modification of Kir2.1*-169C dimeric channels on the properties of block by 100 µM spermine (Fig. 2). For simple comparison between sample traces, pulses to −20 and −10 mV have been highlighted in red and blue, respectively (Fig. 2, A and B). After modification with either compound, the potency of spermine block was reduced (Fig. 2 C). Data were fit with a previously described kinetic model of spermine block (see Materials and methods and Figs. S1 and S2) (Shin and Lu, 2005;

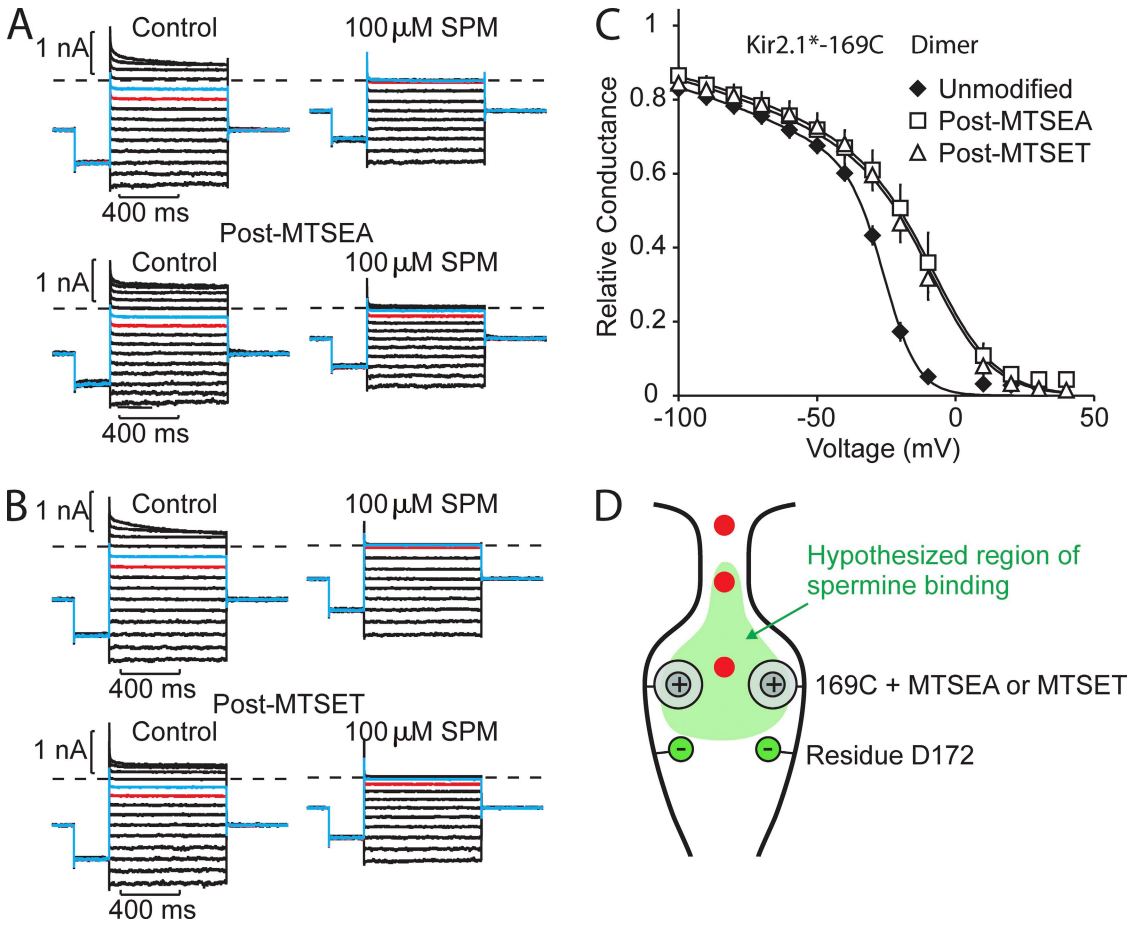

Figure 2. Functional effects of MTSEA and MTSET modification of Kir2.1*-169C dimeric channels. Inside-out patches expressing the Kir2.1*-169C dimer were pulsed between −100 and +50 mV in control or 100 µM spermine. Pulse protocols were repeated after steady-state modification with either (A) MTSEA or (B) MTSET. For simple comparison between control and spermine conditions, pulses to −20 and −10 mV have been highlighted in red and blue, respectively. (C) Conductance–voltage relationships illustrate the voltage dependence of block in control ($n = 13$) or after modification with either MTSEA ($n = 5$) or MTSET ($n = 7$). Mean data were fit with the three-state model described in Materials and methods. (D) Schematic representation of the Kir channel inner cavity, illustrating the spatial relationship between position 169C and the spermine binding site hypothesized from studies in Kir6.2[N160D] channels (Kurata et al., 2006).

Kurata et al., 2007), comprising two sequentially linked binding equilibria, resulting in two distinct components in conductance–voltage relationships (Fig. 2 C). Overall, MTS modification did not substantially affect the shallow spermine binding step, but it significantly reduced the potency and voltage dependence of the deep binding equilibrium. This is evident simply by inspection of conductance–voltage relationships: the shallow voltage-dependent component of spermine block is very similar in control and modified channels, whereas the steep component of block becomes much shallower, and shifted to depolarized voltages, in MTSEA- or MTSET-modified channels (Fig. 2 C). In the context of the kinetic model, this feature is accounted for by a reduction of K2 and a weaker effective valence zδ2 (see supplemental text, Section I, and Fig. S1).

The location of 169C, between the rectification controller (residue D172) and the selectivity filter (Fig. 2 D), overlaps with the deep spermine binding site previously suggested in our studies of Kir6.2[N160D] channels (Kurata et al., 2006, 2008), although more dramatic effects on spermine block were observed after MTSEA modification of the equivalent position (157) in Kir6.2[N160D] (Kurata et al., 2004). This difference in relative sensitivity to modification is generally consistent with the finding that spermine block of Kir2.1 channels is modestly disrupted by charge neutralization of inner cavity residue D172 (Wible et al., 1994; Yang et al., 1995; Guo et al., 2003), whereas high affinity spermine block of Kir6.2[N160D] depends almost entirely on the presence of negative charges in the inner cavity (Shyng et al., 1997; Kurata et al., 2004).

Distinct outcomes of MTSEA and MTSET modification of position 176C

We observed a dramatic difference in the effects of MTSEA versus MTSET on spermine block in Kir2.1*-176C

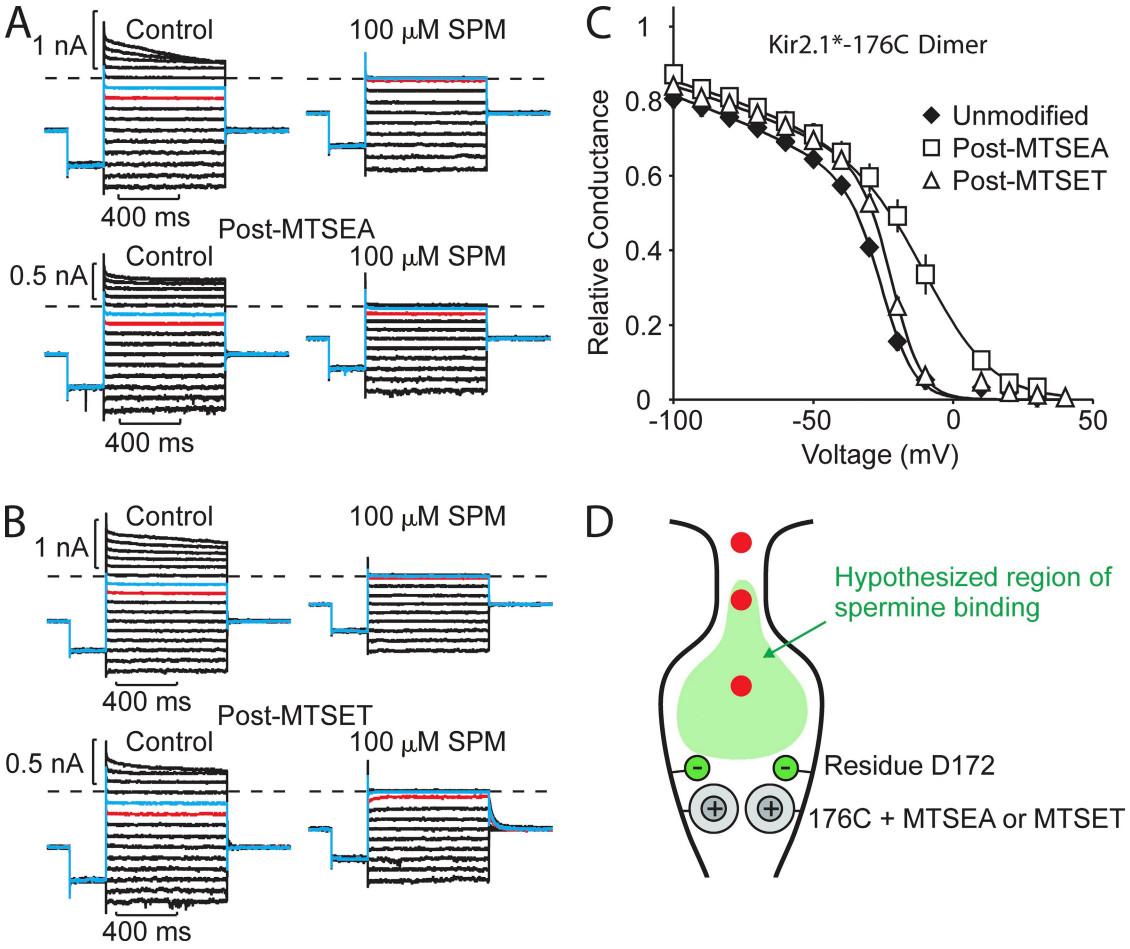

Figure 3. Functional effects of MTSEA and MTSET modification of Kir2.1*-176C dimeric channels. Block by 100 μM spermine was assessed in inside-out patches expressing Kir2.1*-176C dimeric channels, as described in Fig. 2, before and after modification with (A) MTSEA or (B) MTSET. Voltage pulses to −20 and −10 mV are highlighted in red and blue, respectively. (C) Conductance–voltage relationships illustrate the voltage dependence of block in control ($n = 14$), or after modification with either MTSEA ($n = 7$) or MTSET ($n = 7$), and fits are of the three-state model described in Materials and methods. (D) Schematic representation of the Kir channel inner cavity, illustrating the spatial relationship between position 176C and the spermine binding site hypothesized from studies in Kir6.2[N160D] channels (Kurata et al., 2006).

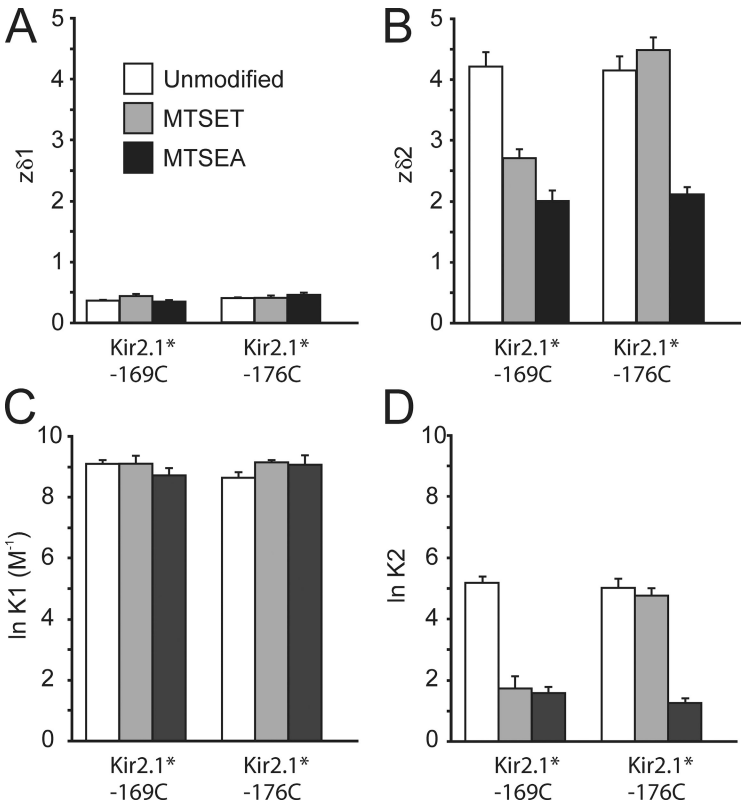

Figure 4. Equilibrium parameters of spermine block in various Kir2.1* dimeric channel constructs. Data from individual patches were fit to a three-site two-barrier model of spermine block (see Materials and methods), comprising two sequentially linked shallow and deep binding sites. Fit parameters describe the effective valence (A and B) and equilibrium constants (C and D) associated with the shallow (zδ1 and K1) and deep (zδ2 and K2) equilibria. Overall, the modification of position 169C or 176 has prominent effects on deep spermine binding (B and D) and very weak effects on shallow binding (A and C). Note the remarkably weak effects of MTSET modification of position 176C.

dimeric channels. MTSEA modification caused a reduction of potency and voltage dependence of the steep component of block (Fig. 3, A and C), similar to that observed in Kir2.1*-169C channels (Fig. 2). However, the effects of MTSET modification of Kir2.1*-176C channels were surprisingly benign, with comparably little effect on steady-state spermine block (Fig. 3, B and C). The voltage dependence of the steep blocking component was unaffected, and only a slight reduction in potency of spermine block was observed (Fig. 3 C). This was especially interesting, as MTSET modification of position 176C, even in dimeric constructs, is more disruptive of conductance (Fig. 1 C). Importantly, whereas 169C overlaps the hypothesized spermine binding site suggested in previous studies of Kir6.2[N160D] channels (Fig. 3 D) (Kurata et al., 2008), 176C is located below the site. The observation that a bulky cationic adduct can be substituted at position 176C, with virtually no effect on steady-state spermine affinity, indicates that this position does not overlap significantly with the spermine binding site (a potential mechanism for the marked difference between MTSEA and MTSET is explored in later sections).

Position and reagent-dependent effects of MTS modification on spermine affinity

Details of fitted equilibrium parameters of block, based on the multistep kinetic model (Scheme 1),

TABLE I

Equilibrium parameters of spermine block before and after modification of dimeric channel constructs

Equilibrium parameter	Unmodified	MTSEA	MTSET
Kir2.1*-176C			
K1 ($*10^3$ M^{-1})	12 ± 1	10 ± 2	9.6 ± 0.7
K2	200 ± 40	3.6 ± 0.5	130 ± 30
zδ1	0.37 ± 0.02	0.44 ± 0.04	0.41 ± 0.04
zδ2	4.2 ± 0.3	2.1 ± 0.1	4.5 ± 0.2
Kir2.1*-169C			
K1 ($*10^3$ M^{-1})	10 ± 1	10 ± 3	7 ± 2
K2	210 ± 30	8 ± 3	5 ± 2
zδ1	0.36 ± 0.02	0.43 ± 0.03	0.33 ± 0.03
zδ2	4.2 ± 0.3	2.7 ± 0.2	2.0 ± 0.3

are summarized in Fig. 4 and Table I. As described, modification of either Kir2.1*-169C or Kir2.1*-176C did not significantly change the effective valence or equilibrium constant of the shallow binding step (Fig. 4, A and C, zδ1 and K1). Rather, channel modification principally affected the deep binding step (corresponding to the steep component of block), reducing the effective valence (zδ2) and binding affinity (K2) in all cases except MTSET modification of Kir2.1*-176C (Fig. 4, B and D). As described, the equilibrium effects of MTSET modification of Kir2.1*-176C channels were weak, with a very small reduction in potency of the deep binding step (4D) and no loss of the effective charge movement associated with blockade (Fig. 4, A and B, zδ1 and zδ2).

These distinct effects of MTSEA and MTSET were further confirmed over a range of spermine concentrations (Fig. 5; presented over a range of voltages in which spermine block is significantly dose dependent). In Kir2.1*-169C dimeric channels (Fig. 5 A), the dose response to spermine is altered significantly by either MTSEA or MTSET modification, and this effect is apparent at multiple voltages. In contrast, the spermine dose–response of Kir2.1*-176C channels is dramatically affected by MTSEA, but only weakly affected by MTSET (Fig. 5 B). In both channel types, the effects of modification become less pronounced at negative voltages, consistent with modification of 169C or 176C predominantly influencing the deep, steeply voltage-dependent spermine binding equilibrium. Model predictions, generated by simultaneous fitting of the entire dataset (spermine concentrations from between 100 to 0.1 μM), are also included (see Table I for fit values), illustrating the utility of the relatively simple Scheme 1 in describing spermine block over a wide range of experimental conditions. Further description of the model is included in the supplemental text (Section I).

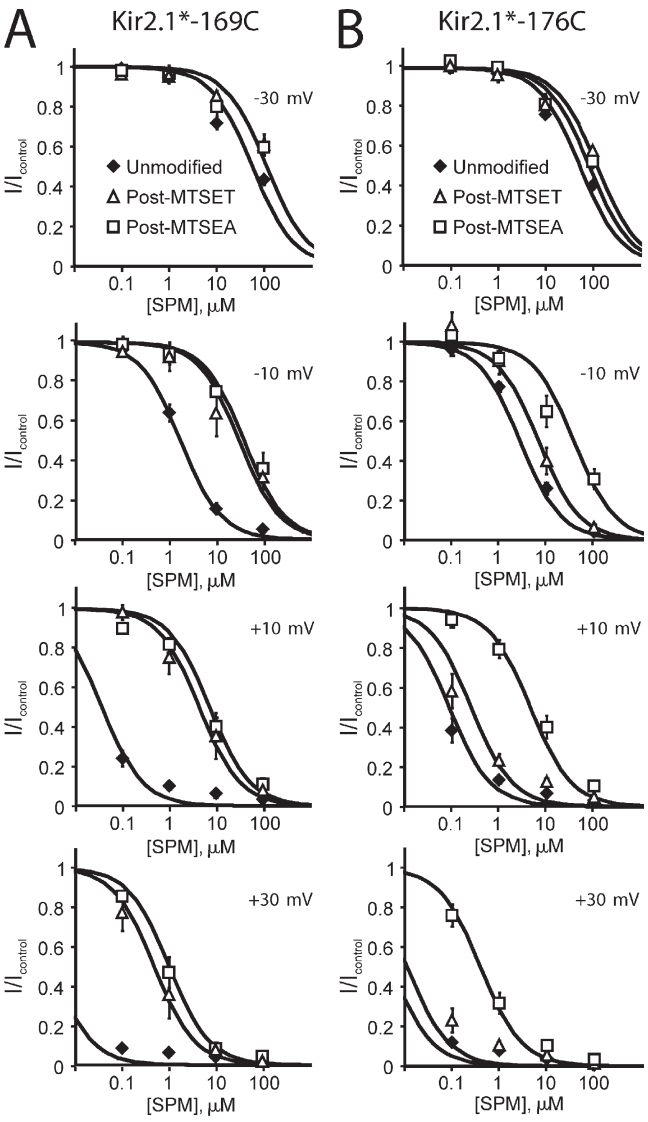

Figure 5. Dose–response curves for spermine block of unmodified and MTSEA- or MTSET-modified channel constructs. Spermine blockade was measured over a range of voltages and concentrations in unmodified and MTSEA- or MTSET-modified (A) Kir2.1*-169C or (B) Kir2.1*-176C channels. Solid lines represent simultaneous fitting of data from all spermine concentrations and voltages to the model described by Scheme 1.

Kinetic effects of MTSET modification at position 176C

The marked position-specific properties of MTSET versus MTSEA modification (176C vs. 169C) suggested localized effects of the charged adduct, rather than a diffuse electrostatic effect of introducing positive charges in the Kir inner cavity. To further explore the local structural perturbation at position 176C, we examined the kinetics of spermine block and unblock of MTSET-modified Kir2.1*-176C in more detail.

Despite modest effects of MTSET modification of Kir2.1*-176C channels on steady-state block, dramatic effects on the kinetics of spermine unbinding were immediately apparent (Fig. 6; also see unblocking kinetics in Fig. 3 B). Unblock of WT Kir2.1 channels is very rapid, and resolution of these kinetics is somewhat limited. However, after MTSET modification of Kir2.1*-176C channels, the kinetics of spermine unblock were slowed significantly (Fig. 6 A), whereas no such slowing was apparent after MTSEA modification. The voltage dependence of spermine unblock rates in MTSET-modified channels (Fig. 6 A, inset) were estimated by plotting $\ln(1/\tau_{off})$ versus voltage and fitting the equation $k_{off}(V) = k_{off}(0\ mV) * e^{(-z\delta FV/RT)}$. The post-MTSET unbinding rate (15 s^{-1} at 0 mV) and voltage dependence (~0.6 elementary charges; Fig. 6 B) were considerably slower and smaller than in WT Kir2.1 channels (280 s^{-1} and ~1.4 elementary charges, published previously; Shin and Lu, 2005; Kurata et al., 2007; with data shown in Fig. 6 B for comparison). Predictions of the kinetic

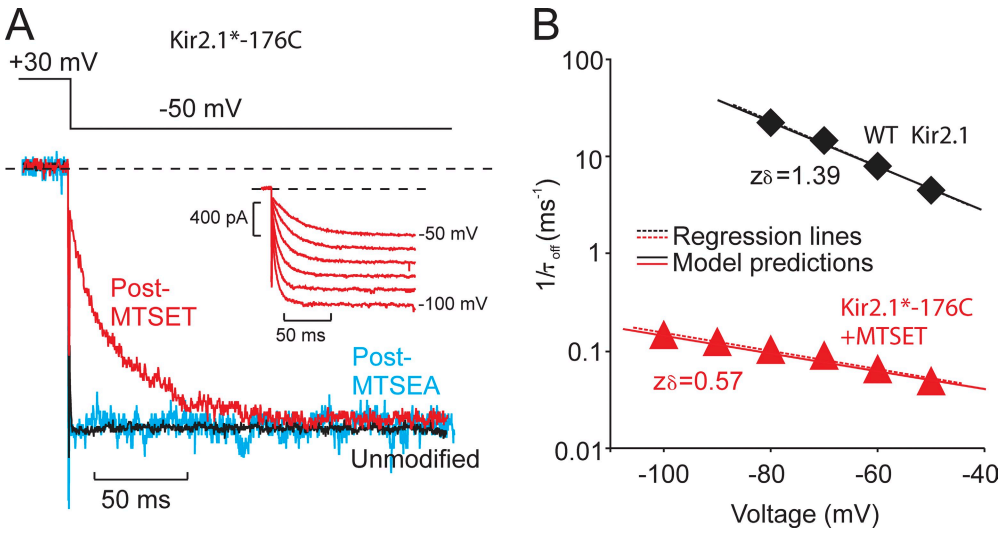

Figure 6. Slow spermine unblock after MTSET modification of Kir2.1*-176C dimeric channels. (A) Pulses from +30 to −50 mV (in 100 µM spermine) illustrate the rate of spermine unblock in unmodified Kir2.1*-176C channels and after modification with either MTSEA (blue) or MTSET (red). Currents are normalized for kinetic comparison. Unblock was dramatically slower in MTSET-modified Kir2.1*-176C channels and was characterized in more detail over a wide voltage range (inset). (B) Mean data illustrating the voltage dependence of spermine unbinding from MTSET-modified Kir2.1*-176C channels ($n = 6$; SEM smaller than symbol size). Straight lines are regression fits and model predictions, as indicated. For comparison, previously determined off-rates from WT Kir2.1 channels are also included, illustrating the relatively shallow voltage dependence of modified channels.

model in Scheme 1 (based on elevation of the barrier between states B1 and B2) are included in Fig. 6 B and closely recapitulate the effects of MTSET modification (176C) on spermine unbinding (see supplemental text, Section II).

Importantly, the appearance of slow unbinding kinetics in MTSET-modified Kir2.1*-176C channels coincides with prepulse voltages lying on the steeply voltage-dependent component of the conductance–voltage relationship (Fig. 7). Voltage pulses that span the range of the shallow blocking component (Fig. 7 A, range ii) do not elicit slow kinetics (Fig. 7 B, ii), whereas prepulses to voltages in the steep range of spermine block elicit a slow component of unbinding that increases with the fraction of channels blocked (Fig. 7 B, i). These data demonstrate that spermine must reach the deep binding site for slow unbinding kinetics to appear. This is consistent with MTSET modification of 176C introducing a barrier for spermine to enter or leave the deep binding site. Elevation of a barrier for blocker migration seems to be a straightforward explanation for the effects of MTSET at position 176C (slowed kinetics, with little effect on spermine affinity).

Spermine blocking kinetics are only subtly affected by MTSET modification of 176C

We also characterized the kinetics of the weakly voltage-dependent spermine blocking step (O→B1), which are apparent in low spermine concentrations. We observed relatively subtle differences between unmodified and MTSET-modified Kir2.1*-176C channels (Fig. 8, A and B). In unmodified channels, we plotted $\ln(1/\tau_{on})$ versus voltage and fit with the equation $k_{on}(V) = k_{on}(0\ mV) * e^{(z\delta FV/RT)}$, yielding a $k_{on}(0\ mV)$ of $3.8*10^6\ M^{-1}s^{-1}$ and effective valence of 0.18. This shallow voltage dependence is consistent with binding to the shallow site acting as a limiting step in blockade, as described previously (Shin et al., 2005; Kurata et al., 2007).

In MTSET-modified Kir2.1*-176C channels, the kinetics of block are comparable to unmodified channels at strong depolarizations (≥+80 mV), but are slightly slower at intermediate voltages (Fig. 8, A, B, and D). This feature at intermediate voltages is also very obvious in higher [spermine] (e.g., 100 µM), where slow kinetics of spermine block are readily apparent in MTSET-modified relative to unmodified 176C channels (Fig. 8 C). Again, predictions deriving from relatively simple modification of the kinetic model in Scheme 1 (elevation of the B1-B2 barrier) reasonably recapitulate the experimental effects of MTSET modification of 176C (Fig. 8 D; see supplemental text, Section II, for a detailed discussion).

Based on simple inspection of the primary data, the effects of MTSET modification of 176C are most easily explained by introduction/elevation of a barrier for spermine migration. This is consistent with the appearance of slowed kinetics together with little or no effect on equilibrium properties of spermine binding. Notably, the experiment introduces a bulky cationic adduct, and so a logical structural interpretation is that spermine must move beyond the bulky adduct to reach the deep spermine binding site. In contrast, if 176C overlapped the spermine binding site (Shin and Lu, 2005; Xu et al., 2009), modification of this residue would be expected to severely disrupt spermine affinity (the interesting difference between MTSEA and MTSET is discussed in subsequent sections). Although this conclusion is apparent from the experimental data, the kinetic model in Scheme 1 can also recapitulate critical details of the experiment, based on changes to the

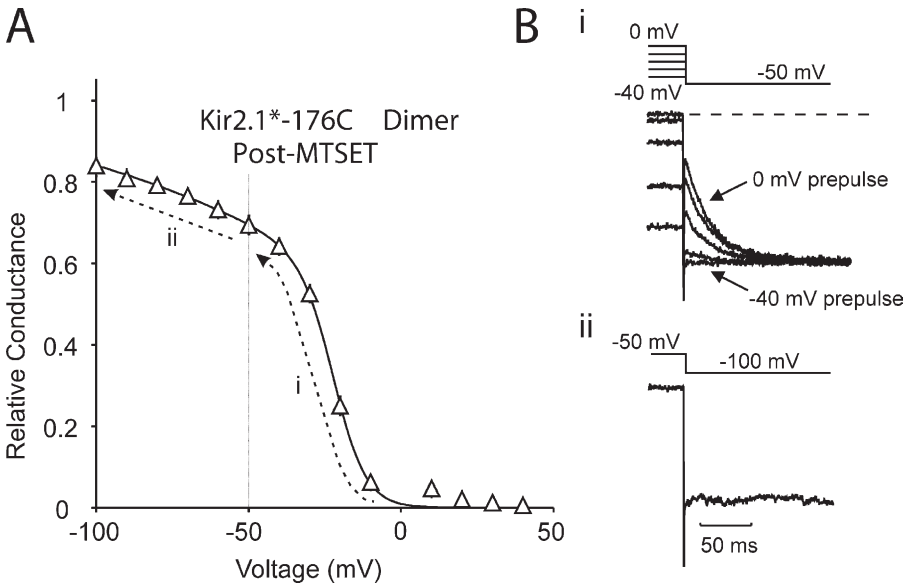

Figure 7. Slow spermine unbinding coincides with the steeply voltage-dependent phase of spermine block. (A) The voltage dependence of spermine block in MTSET-modified Kir2.1*-176C channels is biphasic with a steep range (i) and a shallow voltage range (ii; at voltages below −50 mV). (B) Representative kinetics of blocker unbinding after prepulses to the steeply voltage-dependent range of block (i; −40 to 0 mV) or to voltages in the range of shallow voltage-dependent block (ii). Slow kinetics of spermine unblock develop as a progressively larger fraction of channels are blocked by spermine in the steeply voltage-dependent binding site.

barrier governing the B1–B2 transition (see supplement text, Section II).

Most strikingly, there is little reason to suspect that MTSET modification of 176C (in dimeric channels) significantly affects either the spermine binding site itself or the basic mechanism underlying steeply voltage-dependent block; both spermine affinity and the effective valence of block are virtually unchanged (Figs. 3 and 4, and Table I), and the conductance–voltage relationships in unmodified versus MTSET-modified 176C channels are nearly superimposable. Despite close proximity to the proposed spermine binding site (deep in the inner cavity; Fig. 2 D), the presence of the MTSET adduct is well-tolerated in terms of spermine binding affinity.

Amine–carboxylate interactions in the Kir2.1 inner cavity

The weak equilibrium effects of MTSET modification of 176C on spermine affinity strongly indicate that this position does not overlap with the spermine binding site. However, MTSEA modification of 176C significantly disrupts spermine binding, and we have sought to explain

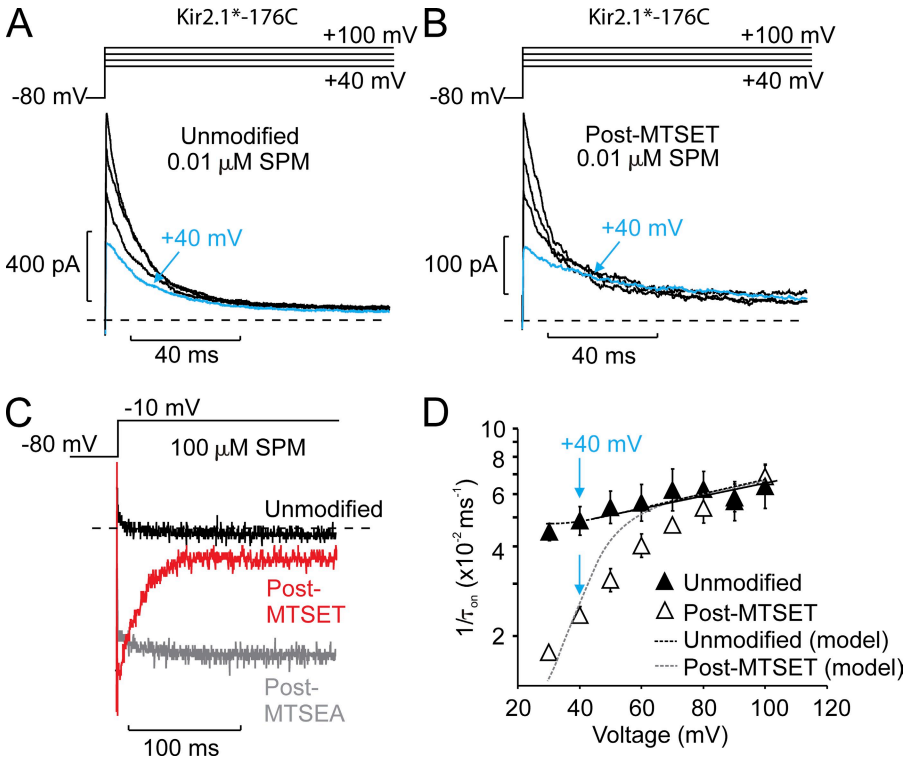

Figure 8. Subtle effects on spermine blocking kinetics after MTSET modification of Kir2.1*-176C channels. Inside-out patches expressing Kir2.1*-176C dimeric channels were pulsed from −80 mV to a range of positive voltages (steps in 20-mV increments are shown for clarity) before (A) and after (B) channel modification with MTSET. Kinetics of block are comparable at positive voltages but slower in MTSET-modified channels at intermediate voltages. (C) Kinetics of spermine block (100 μM) at −10 mV in Kir2.1*-176C channels before and after modification with either MTSEA or MTSET. For comparison, currents have been normalized to the current magnitude at −100 mV in each respective trace. Slow blocking kinetics and more pronounced block are readily apparent in MTSET-modified channels at intermediate voltages. (D) Mean fitted rates of spermine block in Kir2.1*-176C dimeric channels before and after MTSET modification, as determined in 0.01 μM spermine. Straight lines are regression fits or model predictions, as indicated.

this apparent paradox. Because both reagents introduce a positive charge, we speculate that these distinct effects arise from unique chemical properties of each compound. Specifically, the terminal amines of spermine are chemically identical to the primary amine introduced by MTSEA modification. Primary amines are potential hydrogen bond donors and could form close interactions by sharing a proton with the rectification controller (D172) carboxylate side chains. In this way, MTSEA (for which tethering will generate a very high local concentration) might effectively mimic the amines of spermine and compete for interactions with residue D172. Because MTSET introduces a quaternary ammonium, similar interactions with D172 are not possible. In this vein, there are numerous experimental and theoretical findings that indicate fundamentally important differences between quaternary and lower-order ammonium ions in their interactions with carboxylates (Mavri and Vogel, 1994).

We investigated differences in carboxylate interactions with quaternary versus lower-order ammonium ions by testing amine blockers with different degrees of methylation. We compared the effects of two related compounds: DA10, which contains two terminal primary amines, and DQA10, with terminal quaternary amines (Fig. 9 A). In WT Kir2.1 channels, DA10 has higher affinity relative to DQA10, reflected in channel blockade at more negative voltages (Fig. 9, B and C). The D172N mutation disrupts close amine–carboxylate interactions, and this is reflected in a considerable loss of affinity for DA10, but less effect for DQA10. Notably, DA10 and DQA10 become nearly indistinguishable blockers in D172N channels (Fig. 9, D and E) because affinity for DQA10 is relatively less affected by the D172N mutation. This phenomenon likely arises because close ammonium–carboxylate interactions cannot significantly contribute to DQA10 binding in either WT or D172N channels (so the energetic contributions of such an interaction are not lost in the D172N mutant).

To parameterize the distinct interactions of D172 with DA10 and DQA10 blockers, we used lower blocker concentrations, such that the resulting g-V curves were well described with a single Boltzmann function: $I/Io = 1/(1+[blocker]*K_{app}(0\ mV)*e^{(z\delta FV/RT)})$. At lower blocker concentrations, the low affinity shallow binding site is rarely occupied (see Fig. S1), and thus the observed voltage-dependent blockade reflects primarily a distribution between the deep-blocked state and the unblocked

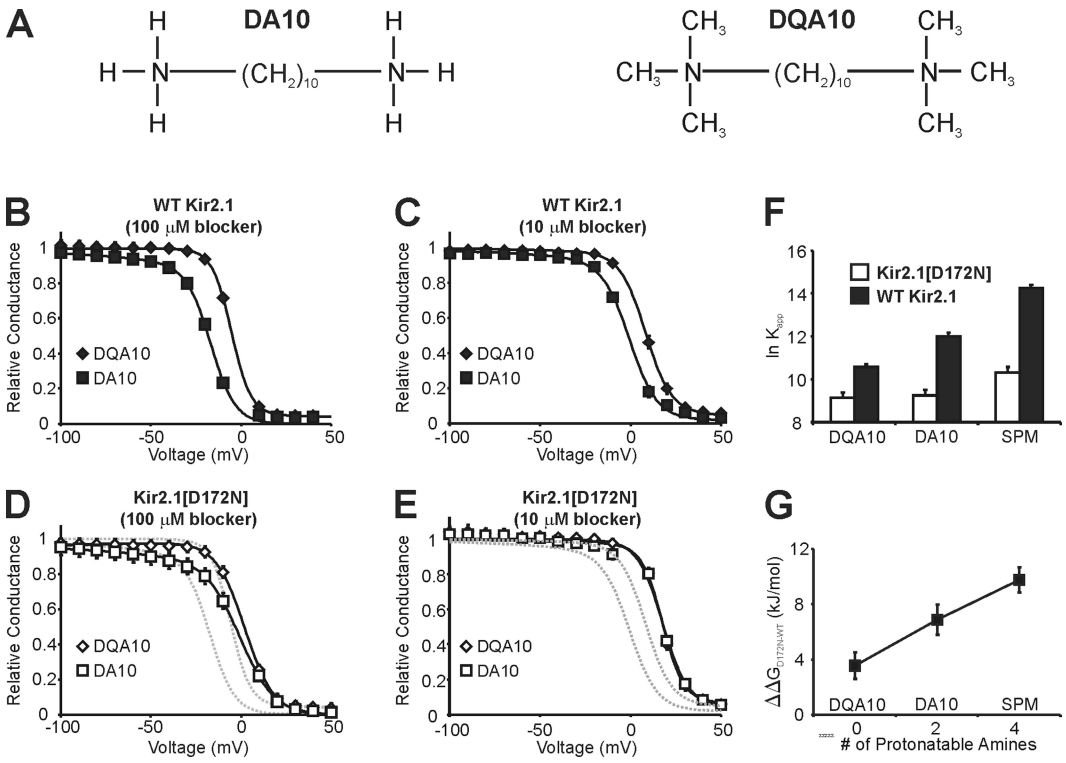

Figure 9. Differential interaction of primary and quaternary ammonium ions with the rectification controller carboxylate. (A) Chemical structures of DA10 and DQA10. (B–E) Steady-state spermine block was characterized as described in Fig. 2, in either 10 or 100 μM spermine for WT Kir2.1 or Kir2.1[D172N] channels, as indicated. (F) K_{app}, reflecting blocker binding to the deep binding site, was determined by fitting a single Boltzmann relationship ($I/I_{control}=1/[1+K_{app}(0\ mV)*e^{(z\delta FV/RT)}]$) to the conductance–voltage relations at low concentrations of each blocker (10 μM for DA10 and DQA10 and 1 μM for spermine). (G) ΔΔG values were determined as $\Delta G_{D172N} - \Delta G_{WT\ Kir2.1,}$ based on the K_{app} constants determined in F. ΔΔG reflects the effect of the D172N mutation on the binding energy of each blocker.

state. This allows a direct comparison of the affinity of each blocker in the deep spermine binding site.

Based on apparent equilibrium constants (K_{app}) derived from blockade in low concentrations (10 µM DA10 and DQA10 and 1 µM spermine; Fig. 9 F), we determined the free energies of binding for each blocker in WT Kir2.1 and D172N and calculated ΔΔG values, reflecting the effect of the D172N mutation on the binding of each blocker (Fig. 9 G). The D172N mutation causes an ∼3.3 kJ/mol reduction in the free energy of binding of DQA10, but nearly double this value (6.4 kJ/mol) for DA10. These differences between DA10 and DQA10 are consistent with stronger interactions of carboxylates with primary ammonium ions relative to quaternary ammonium ions, indicating that specific interactions of primary amines and the D172 carboxylate contribute to high affinity binding. It should be noted that the energy difference between the effects of the D172N mutation on DQA10 versus DA10 binding (∼3.5 kJ/mol) is comparable to a relatively weak hydrogen bond, but it is nevertheless readily observed, with an easily discernable effect on blocker affinity. It is also notable that a comparable increment in binding energy (∼3.2 kJ/mol) is observed for spermine (Fig. 9 G), which comprises two additional protonatable amines versus DA10. However, spermine also has an increased charge relative to DA10 and DQA10, so the extension of the trend to include spermine should be viewed as preliminary and potentially coincidental until a quaternized spermine derivative (with no protonatable amines) is generated and characterized for comparison.

Chemical differences between MTSEA and MTSET underlie their unique functional effects

These observations illustrate a difference between quaternary and lower-order amines in the formation of close ion pairs/hydrogen bonds with carboxylates. We suggest that this difference might underlie the unique effects of MTSEA and MTSET: MTSEA can reduce spermine affinity by closely interacting with D172, whereas MTSET cannot. As depicted schematically in Fig. 10, MTSEA modification of 176C—below the rectification controller—introduces a functional group that mimics spermine and competes for interactions with the D172 carboxylate. Tethering of the modifier leads to a very high effective concentration in the inner cavity, leading to effective competition for interactions required for high affinity spermine binding. In contrast, MTSET introduced at the same position interacts more weakly with the D172 carboxylate (because it is fully methylated), resulting in weaker competition with spermine and a correspondingly smaller effect on spermine affinity. The schematics are intended to depict the important suggestion that MTSEA modification of 176C disrupts spermine block by an indirect mechanism; rather than directly overlapping with the spermine binding site, MTSEA can reduce spermine affinity by engaging the rectification controller carboxylate. We speculate that 176C does not significantly overlap the spermine binding site, and because the chemical properties of MTSET preclude its close interaction with the rectification controller, no indirect effects of this adduct are observed.

DISCUSSION

Altered polyamine block after modification of inner cavity cysteines in Kir2.1

The introduction of positive charges by MTSEA or MTSET modification in the Kir2.1 inner cavity alters spermine potency and kinetics. Unexpectedly, the specific effects of modification depend not only on the location of the substituted cysteine, but also on the chemical properties of the modifying reagent. At position 169C, between the D172 rectification controller and the selectivity filter, modification with either MTSEA or MTSET reduced both the potency and effective valence of spermine block. At position 176C, only ∼10 Å away, MTSEA and MTSET had very different effects: MTSET significantly slowed the unbinding kinetics of spermine, with essentially no effect on blocker affinity, even though MTSET modification of Kir2.1*-176C had the most pronounced effect on channel conductance, reducing currents by nearly 80%. These observations have important implications for localizing the spermine binding site deep in the Kir2.1 inner cavity.

The locale of spermine binding in Kir2.1 channels

The effects of MTS modification are most consistent with a model of polyamine block in which spermine binds between the rectification controller and the selectivity filter, as illustrated by the green "cloud" in Figs. 2 D and 3 D (Kurata et al., 2004, 2006, 2008). We note that neutralization of cytoplasmic residues E224 and E299, distant from the inner cavity, has an effect on rectification by spermine and other blockers (e.g., Mg^{2+}) in Kir2.1 (Yang et al., 1995; Kubo and Murata, 2001; Xie et al., 2002; Guo et al., 2003; Fujiwara and Kubo, 2006). In this regard, recent calculations decomposing the electrostatic contributions of individual residues in the Kir2.1 pore indicate that residues in the cytoplasmic domain (such as E224 and E299) can significantly influence the stability of cations at distant locations, even deep in the inner cavity (Robertson et al., 2008), emphasizing the important point that the effects of mutations are not always local. Interestingly, our findings differ from a very recent report describing perturbing effects of Kir2.1 mutations F174A and I176A on spermine block (Xu et al., 2009). This report is surprising in light of our observation that the introduction of a positively charged side chain in the same

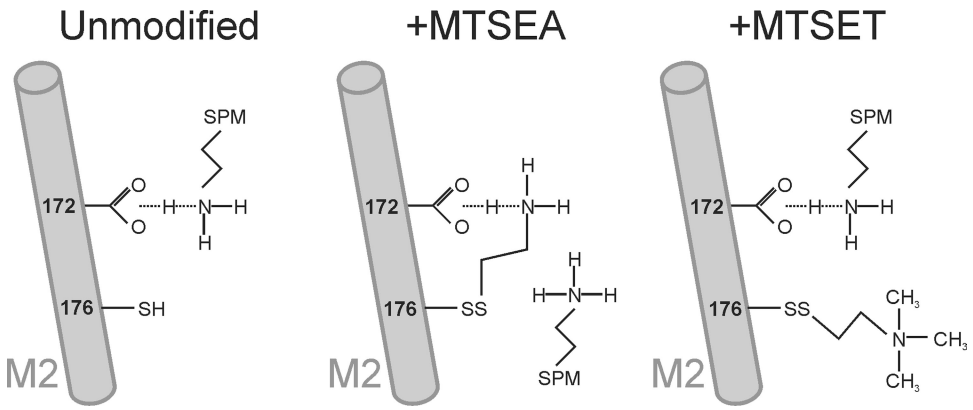

Figure 10. Potential mechanism for differential effects of MTSEA and MTSET modification. In unmodified channels, spermine freely interacts with the D172 carboxylate. In MTSEA-modified 176C channels, MTSEA mimics spermine and competes for strong interactions with the D172 carboxylate. This leads to a reduction in spermine affinity by an indirect mechanism (not by direct overlap with the spermine binding site). MTSET is a quaternary amine and forms much weaker interactions with D172, and therefore does not significantly reduce spermine affinity.

region has little effect on spermine block, and because F174 is not predicted to face the pore. One possible explanation is that these mutations (which significantly disrupt large hydrophobic/aromatic side chains) might act by changing the electrostatics/local dielectric in the locale of D172, although further investigation of these differences clearly seems to be in order.

Here, the introduction of charges overlapping with the proposed spermine binding site, between residue 172 and the selectivity filter, invariably reduces the potency of spermine block (i.e., at position 169C), whereas charge can be introduced just below the rectification controller with dramatic kinetic effects, but little effect on blocker potency. In light of this striking finding, we find it difficult to envision a shallow location of spermine binding that would lead to similar results.

The chemistry of the spermine binding site: a mechanistic basis for differences between MTSEA and MTSET

Differences between MTSEA and MTSET modification at position 176C may reflect the differential interaction of primary versus quaternary amines with the rectification controller carboxylate. Importantly, observations in other biological systems illustrate important differences in the interactions of quaternary amines and lower-order amines with carboxylate side chains. A very informative analogous system is the large body of structural data characterizing the recognition of methylated lysines by proteins involved in histone modification. A notable feature is that lysine methyltransferases selective for lower-order (mono- or di-) methylated lysines often generate specificity by the presence of an aspartate in the active site, which is closely associated (and likely involved in a proton sharing–hydrogen bond interaction) with lysines that are not fully methylated (Taverna et al., 2007).

In the context of K^+ channels, another example of the very weak interaction between quaternary ammonium ions and carboxylates arises in studies of extracellular TEA block, in which the *Shaker* T449E mutant is very insensitive to TEA (Molina et al., 1997). We suspect a similar scenario in our experimental system within the Kir inner cavity. Our findings indicate that primary amines (such as MTSEA or DA10) interact more strongly with the rectification controller carboxylate, relative to quaternary amines (such as MTSET or DQA10). By effectively neutralizing the rectification controller (and competing with the chemically identical amines of spermine), MTSEA can have indirect effects after modification of 176C, with little or no direct spatial overlap with the proposed spermine binding site (Fig. 10).

Given the identical primary amine nature of the terminal amines of spermine and the MTSEA adduct, an obvious extension of our findings is that spermine binding should also involve close interactions of the blocker amines and one or more D172 carboxylates. This is something of a departure from previous discussions of spermine block. Available modeling studies have examined the energetics of spermine (often limited to a fully linearized conformation) or other cations located along the central pore axis (Dibb et al., 2003; Robertson et al., 2008), but the detailed interactions of spermine and the rectification controller (D172) carboxylates have not been explicitly considered. Our findings indicate the importance of the primary amine character of spermine as a determinant of high affinity binding in the inner cavity. Spermine, in addition to being a tetravalent cation, has significant potential to donate hydrogen bonds. With this in mind, the dynamic formation of close ammonium–carboxylate interactions between multiple amines and multiple D172 carboxylates seems entirely plausible as a contributor to high affinity spermine binding in the inner cavity.

Influence of permeant ions on blockade and MTS effects

A final important consideration is the potential impact of permeating ions on the observed effects of MTSEA and MTSET on spermine block. It is both surprising and highly informative that MTSET-modified Kir2.1*-176C channels exhibit no change in the effective valence of spermine block, suggesting that this perturbation has little effect on ion occupancy (at least in ion binding sites that are functionally coupled to spermine blockade). Given that significant perturbation of spermine block is observed with little disruption of current (e.g., MTSEA/ET modification of 169C), whereas strong disruption of current is observed with little reduction of spermine block (e.g., MTSET modification of 176C), we feel it is safe to speculate that the effects of MTSEA and MTSET on spermine block are not significantly determined by indirect effects on ion permeation. Rather, the effects of MTSEA and MTSET (on spermine block) are likely mediated primarily through direct interactions with the blocker (or the D172 side chain). Ideally, a detailed understanding of ion binding sites would contribute to a detailed kinetic model of spermine block, with explicit inclusion of interactions between ions and blockers; however, this remains a significant obstacle in our understanding of Kir channel regulation. It is encouraging that crystallographic studies continue to illuminate this issue (Pegan et al., 2006; Nishida et al., 2007; Tao et al., 2009; Xu et al., 2009), but the distribution of ion binding sites in Kir pores remains unclear. Perhaps more importantly, the effects of voltage on ion distribution are also unclear and may be difficult to establish by crystallography, where no voltage gradient can be applied. The model we have used (see supplemental text) implicitly considers coupled movement of permeant ions (in the effective valence term associated with each rate/equilibrium constant), but it is primarily intended to describe blocker dynamics that can be directly inferred from experimental data.

Conclusions

The modification of cysteines in the inner cavity of Kir2.1 channels provides important constraints on the orientation of the spermine binding site that underlies steeply voltage-dependent channel blockade. MTSET modification of Kir2.1 residue 176C results in a dramatic slowing of the spermine unbinding rate, with little effect on potency or voltage dependence of rectification. This unique and unexpected finding demonstrates that position 176C does not significantly overlap with the spermine binding site, but it can control access to the site when modified with a charged/bulky adduct. This supports the conclusion that the deep spermine binding site predominantly occupies space between the rectification controller (D172) and the selectivity filter. Close interactions between primary amines (in spermine or MTS modifiers) and the rectification controller carboxylates contribute significantly to high affinity spermine binding.

We thank Ru-Chi Shieh (Institute of Biomedical Sciences, Taipei, Taiwan) for kindly providing the IRK1J (Kir2.1*) background construct.

This work was supported by National Institutes of Health (NIH) grant HL53268 and a National Sciences and Engineering Research Council of Canada Discovery Grant to H.T. Kurata, and NIH grant HL52670 to C.G. Nichols.

Lawrence G. Palmer served as editor.

Submitted: 1 May 2009
Accepted: 12 April 2010

REFERENCES

Bianchi, L., M.L. Roy, M. Taglialatela, D.W. Lundgren, A.M. Brown, and E. Ficker. 1996. Regulation by spermine of native inward rectifier K+ channels in RBL-1 cells. *J. Biol. Chem.* 271:6114–6121. doi:10.1074/jbc.271.11.6114

Chang, H.K., S.H. Yeh, and R.C. Shieh. 2005. A ring of negative charges in the intracellular vestibule of Kir2.1 channel modulates K+ permeation. *Biophys. J.* 88:243–254. doi:10.1529/biophysj.104.052217

Colquhoun, D., and A.G. Hawkes. 1995. A Q-matrix cookbook: how to write only one program to calculate the single-channel and macroscopic predictions for any kinetic mechanism. *In* Single Channel Recording. B. Sakmann and E. Neher, editors. Plenum Press, New York. 589–636.

Dibb, K.M., T. Rose, S.Y. Makary, T.W. Claydon, D. Enkvetchakul, R. Leach, C.G. Nichols, and M.R. Boyett. 2003. Molecular basis of ion selectivity, block, and rectification of the inward rectifier Kir3.1/Kir3.4 K(+) channel. *J. Biol. Chem.* 278:49537–49548. doi:10.1074/jbc.M307723200

Fakler, B., U. Brändle, E. Glowatzki, S. Weidemann, H.P. Zenner, and J.P. Ruppersberg. 1995. Strong voltage-dependent inward rectification of inward rectifier K+ channels is caused by intracellular spermine. *Cell.* 80:149–154. doi:10.1016/0092-8674(95)90459-X

Ficker, E., M. Taglialatela, B.A. Wible, C.M. Henley, and A.M. Brown. 1994. Spermine and spermidine as gating molecules for inward rectifier K+ channels. *Science.* 266:1068–1072. doi:10.1126/science.7973666

Fujiwara, Y., and Y. Kubo. 2006. Functional roles of charged amino acid residues on the wall of the cytoplasmic pore of Kir2.1. *J. Gen. Physiol.* 127:401–419. doi:10.1085/jgp.200509434

Guo, D., and Z. Lu. 2000. Mechanism of IRK1 channel block by intracellular polyamines. *J. Gen. Physiol.* 115:799–814. doi:10.1085/jgp.115.6.799

Guo, D., Y. Ramu, A.M. Klem, and Z. Lu. 2003. Mechanism of rectification in inward-rectifier K^+ channels. *J. Gen. Physiol.* 121:261–275. doi:10.1085/jgp.200208771

John, S.A., L.H. Xie, and J.N. Weiss. 2004. Mechanism of inward rectification in Kir channels. *J. Gen. Physiol.* 123:623–625. doi:10.1085/jgp.200409017

Kubo, Y., and Y. Murata. 2001. Control of rectification and permeation by two distinct sites after the second transmembrane region in Kir2.1 K+ channel. *J. Physiol.* 531:645–660. doi:10.1111/j.1469-7793.2001.0645h.x

Kurata, H.T., L.R. Phillips, T. Rose, G. Loussouarn, S. Herlitze, H. Fritzenschaft, D. Enkvetchakul, C.G. Nichols, and T. Baukrowitz. 2004. Molecular basis of inward rectification: polyamine interaction

sites located by combined channel and ligand mutagenesis. *J. Gen. Physiol.* 124:541–554. doi:10.1085/jgp.200409159

Kurata, H.T., L.J. Marton, and C.G. Nichols. 2006. The polyamine binding site in inward rectifier K^+ channels. *J. Gen. Physiol.* 127:467–480. doi:10.1085/jgp.200509467

Kurata, H.T., W.W. Cheng, C. Arrabit, P.A. Slesinger, and C.G. Nichols. 2007. The role of the cytoplasmic pore in inward rectification of Kir2.1 channels. *J. Gen. Physiol.* 130:145–155. doi:10.1085/jgp.200709742

Kurata, H.T., K. Diraviyam, L.J. Marton, and C.G. Nichols. 2008. Blocker protection by short spermine analogs: refined mapping of the spermine binding site in a Kir channel. *Biophys. J.* 95:3827–3839. doi:10.1529/biophysj.108.133256

Lopatin, A.N., E.N. Makhina, and C.G. Nichols. 1994. Potassium channel block by cytoplasmic polyamines as the mechanism of intrinsic rectification. *Nature.* 372:366–369. doi:10.1038/372366a0

Lopatin, A.N., E.N. Makhina, and C.G. Nichols. 1995. The mechanism of inward rectification of potassium channels: "long-pore plugging" by cytoplasmic polyamines. *J. Gen. Physiol.* 106:923–955. doi:10.1085/jgp.106.5.923

Lopatin, A.N., L.M. Shantz, C.A. Mackintosh, C.G. Nichols, and A.E. Pegg. 2000. Modulation of potassium channels in the hearts of transgenic and mutant mice with altered polyamine biosynthesis. *J. Mol. Cell. Cardiol.* 32:2007–2024. doi:10.1006/jmcc.2000.1232

Lu, T., B. Nguyen, X. Zhang, and J. Yang. 1999. Architecture of a K+ channel inner pore revealed by stoichiometric covalent modification. *Neuron.* 22:571–580. doi:10.1016/S0896-6273(00)80711-4

Mavri, J., and H.J. Vogel. 1994. Ion pair formation involving methylated lysine side chains: a theoretical study. *Proteins.* 18:381–389. doi:10.1002/prot.340180408

Molina, A., A.G. Castellano, and J. López-Barneo. 1997. Pore mutations in Shaker K+ channels distinguish between the sites of tetraethylammonium blockade and C-type inactivation. *J. Physiol.* 499:361–367.

Nishida, M., M. Cadene, B.T. Chait, and R. MacKinnon. 2007. Crystal structure of a Kir3.1-prokaryotic Kir channel chimera. *EMBO J.* 26:4005–4015. doi:10.1038/sj.emboj.7601828

Pegan, S., C. Arrabit, P.A. Slesinger, and S. Choe. 2006. Andersen's syndrome mutation effects on the structure and assembly of the cytoplasmic domains of Kir2.1. *Biochemistry.* 45:8599–8606. doi:10.1021/bi060653d

Priori, S.G., S.V. Pandit, I. Rivolta, O. Berenfeld, E. Ronchetti, A. Dhamoon, C. Napolitano, J. Anumonwo, M.R. di Barletta, S. Gudapakkam, et al. 2005. A novel form of short QT syndrome (SQT3) is caused by a mutation in the KCNJ2 gene. *Circ. Res.* 96:800–807. doi:10.1161/01.RES.0000162101.76263.8c

Robertson, J.L., L.G. Palmer, and B. Roux. 2008. Long-pore electrostatics in inward-rectifier potassium channels. *J. Gen. Physiol.* 132:613–632. doi:10.1085/jgp.200810068

Schulze-Bahr, E. 2005. Short QT syndrome or Andersen syndrome: Yin and Yang of Kir2.1 channel dysfunction. *Circ. Res.* 96:703–704. doi:10.1161/01.RES.0000164186.86838.09

Shin, H.G., and Z. Lu. 2005. Mechanism of the voltage sensitivity of IRK1 inward-rectifier K^+ channel block by the polyamine spermine. *J. Gen. Physiol.* 125:413–426. doi:10.1085/jgp.200409242

Shin, H.G., Y. Xu, and Z. Lu. 2005. Evidence for sequential ion-binding loci along the inner pore of the IRK1 inward-rectifier K^+ channel. *J. Gen. Physiol.* 126:123–135. doi:10.1085/jgp.200509296

Shyng, S., T. Ferrigni, and C.G. Nichols. 1997. Control of rectification and gating of cloned KATP channels by the Kir6.2 subunit. *J. Gen. Physiol.* 110:141–153. doi:10.1085/jgp.110.2.141

Tao, X., J.L. Avalos, J. Chen, and R. MacKinnon. 2009. Crystal structure of the eukaryotic strong inward-rectifier K+ channel Kir2.2 at 3.1 A resolution. *Science.* 326:1668–1674. doi:10.1126/science.1180310

Taverna, S.D., H. Li, A.J. Ruthenburg, C.D. Allis, and D.J. Patel. 2007. How chromatin-binding modules interpret histone modifications: lessons from professional pocket pickers. *Nat. Struct. Mol. Biol.* 14:1025–1040. doi:10.1038/nsmb1338

Wible, B.A., M. Taglialatela, E. Ficker, and A.M. Brown. 1994. Gating of inwardly rectifying K+ channels localized to a single negatively charged residue. *Nature.* 371:246–249. doi:10.1038/371246a0

Xie, L.H., S.A. John, and J.N. Weiss. 2002. Spermine block of the strong inward rectifier potassium channel Kir2.1: dual roles of surface charge screening and pore block. *J. Gen. Physiol.* 120:53–66. doi:10.1085/jgp.20028576

Xie, L.H., S.A. John, and J.N. Weiss. 2003. Inward rectification by polyamines in mouse Kir2.1 channels: synergy between blocking components. *J. Physiol.* 550:67–82. doi:10.1113/jphysiol.2003.043117

Xu, Y., H.G. Shin, S. Szep, and Z. Lu. 2009. Physical determinants of strong voltage sensitivity of K(+) channel block. *Nat. Struct. Mol. Biol.* 16:1252–1258.

Yang, J., Y.N. Jan, and L.Y. Jan. 1995. Control of rectification and permeation by residues in two distinct domains in an inward rectifier K+ channel. *Neuron.* 14:1047–1054. doi:10.1016/0896-6273(95)90343-7